

RESEARCH ARTICLE | OCTOBER 01 1978

## Effect of transonic flow in the ablation cloud on the lifetime of a solid hydrogen pellet in a plasma

P. B. Parks; R. J. Turnbull



*Phys. Fluids* 21, 1735–1741 (1978)  
<https://doi.org/10.1063/1.862088>



View  
Online



Export  
Citation

CrossMark

18 January 2024 10:08:07

## AML Machine Learning WEBINAR

Fostering a New Data Culture with *APL Machine Learning*



12:00PM (noon) EST



Thursday, January 18, 2024

Moderated by:  
Adnan Mehonic



# Effect of transonic flow in the ablation cloud on the lifetime of a solid hydrogen pellet in a plasma

P. B. Parks<sup>a)</sup> and R. J. Turnbull

Department of Electrical Engineering, University of Illinois, Urbana, Illinois 61801  
(Received 28 April 1977; final manuscript received 26 May 1978)

A knowledge of solid hydrogen pellet lifetimes in a plasma is critical to the design of devices to refuel tokamak fusion reactors. When the pellet is injected into the plasma, the ablated material from the pellet undergoes a transonic flow since it is heated while it expands. Calculations are done on the behavior of the transonic flow for various plasma conditions and pellet sizes. From these calculations, the ablation rate and lifetimes of the pellet are determined. A scaling law is given which allows pellet lifetimes to be easily calculated for any plasma conditions. The results of these calculations give good agreement when compared with experiments.

## I. INTRODUCTION

Frozen pellets of deuterium and tritium are being proposed as the means of refueling nuclear fusion reactors of the tokamak configuration.<sup>1</sup> In order to assess the viability of this method of refueling, it is necessary to determine the pellet lifetime in a plasma. In this paper we improve an earlier model concerning the plasma-pellet ablation problem.<sup>2</sup> Reference 2 also contains a summary of previous work in this area which will not be repeated here.

The basic physical phenomena to be considered are the following: Electrons from the plasma impact on the pellet surface, thus heating it. The heated pellet surface begins to ablate neutral molecules. These neutral molecules form a dense ablation cloud around the pellet surface partially shielding it from the plasma energy flux. Under most plasma conditions of interest (densities greater than  $10^{12} \text{ cm}^{-3}$ ) the incident plasma electrons deposit almost all of their energy in the ablatant through elastic backscattering and inelastic processes. Thereby, the sum of the ablation enthalpy and flow kinetic energy is raised to over an order of magnitude higher than the energy required to vaporize the solid (0.01 eV/molecule). Thus, it follows that the energy flux striking the surface of the pellet and the vaporization energy are both negligible. For this reason, the dynamics of the ablatant flow, in particular, this "self-shielding" effect, are more important in controlling the ablation rate than the details of the phase transition at the pellet surface.

In the ablation cloud it appears that two basic phenomena are in simultaneous operation: heating, which predominates near the pellet, and expansion, which predominates in the outer, more tenuous portion of the cloud. This combination of heating and radial flow ought to produce an effect equivalent to that of the walls in a convergent-divergent nozzle.<sup>3</sup> We expect that the flow, beginning at the pellet surface, is subsonic and is accelerated continuously up to a sonic radius, at which point the effects of heating and area increase exactly balance and the flow becomes supersonic. It will be

seen that the effect of the back pressure due to the surrounding plasma is negligible, so that supersonic flow of the ablation cloud can actually be realized until a shock front is reached. At the shock front, the ablation cloud suddenly becomes subsonic in order that the proper pressure boundary condition is reached as  $r \rightarrow \infty$ . This shock front is so far from the pellet that it essentially has no effect on the shielding. This "nozzling" effect of an ablation flow has also been considered in Ref. 4 for a laser-driven implosion problem.

Quasi-steady conditions are assumed since the time scale for the establishment of the ablation cloud (the pellet radius divided by the ablation cloud velocity) is much shorter than the pellet lifetime, typical values for the times are  $10^{-7}$  sec to establish the ablation cloud and  $10^{-5}$  to  $10^{-4}$  sec for the pellet lifetime. In addition, the total integrated thickness of the ablation cloud is finite for a spherical expansion in the steady state; therefore, the pellet will ablate at a rate determined by its instantaneous radius (and instantaneous external plasma parameters if they vary slowly enough).

In the earlier model,<sup>2</sup> called the "sonic approximation," it was assumed that the flow was sonic throughout the entire ablation cloud. In addition, instead of solving for the incident electron energy flux at each point in the cloud an artificial "shape factor" was fashioned on the basis of a constant electron particle flux and constant electron loss function,  $L(E)$ , in the ablation cloud in connection with its heating. It was useful primarily in obtaining the total integrated ablation cloud thickness so that the energy flux at the pellet surface could be obtained in a self-consistent manner. Despite these obvious deficiencies in the sonic approximation the correctness of the resulting scaling laws for the pellet lifetime and temperature in the ablation cloud can be demonstrated by using the more complete model presented in this paper.

Looking ahead, under conditions projected for fusion reactors the ablation cloud conditions predicted by this model at the sonic transition point are a temperature of 1–2 eV and a density of  $10^{19}$  to  $10^{20} \text{ cm}^{-3}$ . Taking these conditions as typical allows several approximations in the equations. The heat flux due to thermal

<sup>a)</sup>Current address: General Atomic Company, San Diego, Calif. 92138.

heat conduction within the ablation cloud can be ignored because it is a few orders of magnitude less than the energy flux of the degraded incident electrons. The viscosity effects on the flow can also be ignored because the characteristic Reynolds number at  $r_*$  (the sonic transition radius) is extremely large.

For the gasdynamic expansion we assume an inviscid perfect gas with constant specific heat. The neglect of thermal dissociation and ionization in the ablation is an obvious limitation of the model. Further refinements to include ionization and dissociation have recently been carried out,<sup>5,6</sup> but they introduce numerical complexities which are beyond the scope of this paper. However, we wish to point out that these atomic processes only reduce the ablation rate by about 20%; furthermore, the transonic behavior of the flow and the scaling laws derived in this paper are not altered substantially.

Other considerations pertaining to the plasma-pellet ablation problem are electrostatic charging and magnetic field effects. As discussed briefly in Ref. 2 the thermalized electrons in the ablation cloud give rise to a "return current" that balances the current of the incoming fast incident electrons under quasi-equilibrium. A self-consistent electric field arises which may inhibit the incident electron energy flux and simultaneously give rise to Ohmic heating. If we take quantities at the sonic radius as representative of the ablation cloud, the effect of the electric field can be estimated by using Ohm's law

$$\epsilon_* = en_{e0}v_{e0}/4\sigma_*,$$

where  $\epsilon_*$  is the electric field,  $e$  is the electronic charge,  $n_{e0}$  is the plasma electron density,  $v_{e0}$  is the average plasma electron velocity,  $en_{e0}v_{e0}/4$  is the incident electron current at a large radius and is on the order of the "return current" at the sonic radius, and  $\sigma_*$  is the electrical conductivity of the ablation cloud at the sonic radius. An asterisk is used to denote quantities at the sonic transition point. The electrostatic potential,  $\phi_p$ , in the ablation cloud is of the order of  $\epsilon_* r_*$  or since  $r_*$  is less than two pellet radii,  $\phi_p$  is approximately

$$(300en_{e0}v_{e0}/4\sigma_*)r_p \text{ (volts)},$$

where  $r_p$  is the pellet radius. For a partially ionized hydrogen gas, we include the effect of electron-neutral collisions to get a simple expression for the electrical conductivity,  $\sigma_*$

$$\sigma_* = \frac{f_{i*}}{3.4 \times 10^{-16}(1-f_{i*})T_*^{1/2} + 5.8 \times 10^{-15} \ln \Lambda f_{i*} T_*^{-3/2}},$$

where  $f_{i*}$  is the fraction of the cloud which is ionized at the sonic radius,  $T_*$  is the temperature of the ablation cloud at the sonic radius, and  $\Lambda = 3.6 \times 10^9 T_*^{3/2}/n_{e0}^{1/2}$ , where  $n_{e0}$  is the electron density at the sonic radius. This expression is confirmed by experimental and theoretical results.<sup>7</sup> One expects to find that the electrostatic potential becomes weaker as the amount of ionization in the ablation cloud increases. For example, under fusion conditions,  $n_{e0} = 10^{14} \text{ cm}^{-3}$ ,  $T_{e0} = 10 \text{ keV}$ , and  $r_p = 0.1 \text{ cm}$  one obtains from the scaling laws derived in this paper that for deuterium pellets (assuming the ratio of specific heat is  $\frac{5}{3}$ ) the temperature at the sonic

radius  $T_* = 1.26 \text{ eV}$  and the total particle density in the ablation cloud at that point is  $n_* = 1.78 \times 10^{20} \text{ cm}^{-3}$ . These quantities determine the thermal ionization fraction in the ablation cloud. Using the Saha equilibrium equation<sup>8</sup> which is valid for local thermodynamic equilibrium (which certainly exists because the atomic collision time scale is much smaller than the hydrodynamic time scale  $r_*/v_*$  where  $v_*$  is the velocity at the sonic transition point), we find that this fraction, denoted by  $f_{i*}$ , is 0.022.

Taking  $\ln \Lambda = 2.5$ , the electrical conductivity  $\sigma_* = 3.7 \times 10^{13} \text{ sec}^{-1}$  giving, for the electrostatic potential,  $\phi_p = 60 \text{ V}$  which is negligible compared with the incident electron energy of approximately 10 keV so the incident electrons are not slowed down appreciably by the electrostatic fields. Clearly, Ohmic heating is negligible compared with heating by the degradation of the incident electron energy flux in the ablation cloud. One probably expects stronger fields nearer the pellet surface where the ablation temperature is lower and hence  $f_{i*}$  is lower. For this reason, the charging aspect of the plasma-pellet ablation deserves further analysis, but in this paper it is omitted, because it appears to be negligible.

Due to the finite conductivity of the ablation cloud a possible distortion of the magnetic field in the vicinity of the pellet could alter the transport of the incident electrons which are assumed to follow the straight magnetic lines which thread the pellet and ablation cloud. Even a nonspherical expansion is possible if the lines are distorted and the flow is significantly ionized. There are two conditions which should be met if magnetic field effects are to play a role in the ablation dynamics. First, the characteristic magnetic Reynolds number of the ablation cloud,  $R_{mk} = (4\pi v_* \sigma_* r_*)/c^2$  (where  $c$  is the speed of light), must be at least of order one in order that the outward ablation flow velocity exceed the velocity of the inward diffusion of the magnetic field lines. Second, the ratio of the pressure of the ablation cloud to the magnetic-field pressure  $\beta_* = p_*/(B^2/8\pi)$  should be at least one ( $p_*$  is the ablation cloud pressure at the sonic radius and  $B$  is the magnetic flux density). For a magnetic field strength of 25 kG and taking the fusion conditions given here, we find from the scaling laws that  $R_{mk} = 0.1$  and  $\beta_* = 14$ . For larger pellets and/or plasma densities the temperature at the sonic radius will be higher leading to larger values of  $f_{i*}$  and  $\sigma_*$ . Therefore, the omission of magnetic field effects appears to be valid if we consider pellets of about 0.1 cm or less and plasma densities of  $10^{14} \text{ cm}^{-3}$  or less.

A summary of the physics of the problem is as follows: The incident plasma electrons deposit their energy in the ablation cloud with a very small amount of energy reaching the pellet surface. There is no appreciable electric field to retard the electrons because the small amount of ionization produced in the ablation cloud acts to prevent any large electric field. The ablation cloud undergoes a continuously heated expansion. Under conditions of temperature and density up to those projected for fusion reactors, the ionization of the ablation cloud occurs at a large enough radius so that it has a very small effect on the shielding. Although dissociation takes place in the ablation cloud, it is a relatively small

effect and therefore is not included. Finally, any distortion of the magnetic field by the ablation cloud, resulting in a reduced incident energy flux, is neglected because it would only be important in very dense plasmas.

## II. DEVELOPMENT OF THE EQUATIONS

Incident plasma electrons encountering the ablation cloud of the pellet lose energy through inelastic processes such as ionization and excitation of the neutral hydrogen molecules and/or atoms and simultaneously undergo elastic scattering. Both effects degrade the total incident electron energy flux providing a thermal energy flux providing a thermal energy source to the ablation cloud expansion. Assuming that Maxwell-Boltzmann statistics apply for the plasma electrons far away from the pellet which have temperature  $T_{e0}$  and density  $n_{e0}$ , then the unattenuated electron energy flux  $q_0$ , is

$$q_0 = (n_{e0} v_{e0}/4) E_0, \quad (1)$$

where  $v_{e0} = (8kT_{e0}/\pi m_e)^{1/2}$ ,  $E_0 = 2kT_{e0}$ ,  $m_e$  is the electron mass, and  $k$  is the Boltzmann constant.

As an approximation, the distribution of electrons is replaced with an equivalent mono-energetic flux of electrons with average energy  $E_0$ . Assuming that these mono-energetic electrons lose their energy continuously as they enter the ablation cloud, a relation between the distance an electron travels along the magnetic field and its energy is given by

$$dE/dr = \rho(r) L(E)/m \langle \cos\theta \rangle, \quad (2)$$

where  $\rho(r)$  is the mass density of the ablatant,  $m$  is the average mass of an ablatant species, and  $L(E)$  is the energy dependent loss function. The  $\langle \cos\theta \rangle$  term accounts for the average pitch angle of the electrons with respect to the magnetic field which, if weighted with an assumed isotropic distribution, is approximated by 1/2.

The equation governing the incident electron energy flux,  $q$ , at a point  $r$  in the ablation cloud is, in the mono-energetic approximation,

$$q(r) = q_0 \frac{E(r)}{E_0} \exp \left[ \int_{E(r)}^{E_0} 1/2\hat{\sigma}_T(E') L(E')^{-1} dE' \right], \quad (3)$$

where  $\hat{\sigma}_T(E)$  is the effective backscattering cross section which includes small angle scattering as well as single event backscattering. Its derivation is in Ref. 2 which made use of the differential elastic scattering cross section for electrons or atomic hydrogen based on the Börn approximation. It was then adjusted to reflect the experimentally determined values for the total elastic scattering cross section<sup>9</sup> and is given by

$$\hat{\sigma}_T(E) = \begin{cases} \frac{8.8 \times 10^{-13}}{E^{1.71}} - \frac{1.62 \times 10^{-12}}{E^{1.332}}; & E > 100 \text{ eV}, \\ \frac{1.1 \times 10^{-14}}{E}; & E < 100 \text{ eV}. \end{cases}$$

Electrons which are turned around (backward flux) by elastic collisions are no longer considered, because their contribution to the total energy flux is small; the "double backscattering" process reduces their energy

to essentially zero. This assumption has been verified by Monte Carlo calculations for electrons streaming through molecular hydrogen gas.<sup>10</sup> It is assumed that the energy of these electrons is transferred to the cloud at the point where they are backscattered.

The electron loss function,  $L(E)$ , used in Eqs. (2) and (3), has been studied extensively for molecular hydrogen by Miles *et al.*<sup>11</sup> who obtained accurate semi-empirical cross sections for the discrete excitation, ionization, and dissociation processes. In this way  $L(E)$  can be constructed from a knowledge of the various individual cross sections which characterize the inelastic collisions. Miles fitted  $L(E)$  to a versatile expression which is accurate down to 20 eV, viz.,

$$L(E) = 8.62 \times 10^{-15}$$

$$\times \left[ \left( \frac{E}{100} \right)^{0.823} + \left( \frac{E}{60} \right)^{-0.125} + \left( \frac{E}{48} \right)^{-1.94} \right]^{-1} \text{ eV-cm}^2.$$

The dynamics of the ablation cloud are given by the equations of conservation of mass, momentum, and energy and the equation of state for a perfect gas with constant specific heat. These equations are a spherically symmetric expansion

$$\rho v r^2 = G/4\pi, \quad (4)$$

$$\rho v dv/dr + dp/dr = 0, \quad (5)$$

$$\frac{G}{4\pi r^3} \frac{d}{dr} \left( \frac{\gamma k T}{(\gamma - 1)m} + \frac{v^2}{2} \right) = Q \frac{dq}{dr}, \quad (6)$$

where  $m$  is the average particle mass of the ablatant,  $v$  is the flow velocity,  $p$  is the pressure,  $T$  is the temperature,  $\gamma$  is the ratio of specific heat, and  $G$  is the ablation rate in g/sec.  $Q$  is the fraction of the electron energy loss,  $dq/dr$ , which goes into heating the cloud. Its value is approximately 0.6–0.7<sup>5</sup> and is, for simplicity, assumed to be a constant at all points in the cloud.

The heat flow equation must be supplemented by a relation governing  $dq/dr$ . Using Eq. (3) in conjunction with Eq. (2) yields

$$dq/dr = (\rho/m) q \Lambda(E) \quad (7)$$

where  $\Lambda(E) = \hat{\sigma}_T(E) + 2L(E)/E$  can be regarded as an "effective" energy flux cross section. Equations (2), (4), (5), (6), (7), and the equation of state comprise the system of equations of interest in this problem.

The boundary conditions necessary to determine the solution are that the electron energy and energy flux must approach that of the plasma as  $r \rightarrow \infty$  and the pressure in the ablation cloud must go to zero as  $r \rightarrow \infty$ . At the pellet surface, the electron energy flux goes into heating the pellet surface, supplying the heat of vaporization for the ablating molecules, and providing the initial energy of the ablation cloud. The rate of ablation depends on the surface temperature of the pellet. For plasmas of fusion interest the amount of energy flux that actually strikes the pellet surface is insignificant compared with the energy flux deposited in the ablation cloud. Also, the temperature of the ablation cloud at the pellet surface is much smaller than it is at the sonic

radius so we will take it as zero. The boundary conditions can therefore be written as

$$p \rightarrow 0 \quad (8)$$

$$q \rightarrow q_0, \quad E \rightarrow E_0 \quad (9)$$

and the surface boundary conditions become

$$q(r_p) = 0, \quad T(r_p) = 0. \quad (10)$$

### III. SOLUTIONS TO THE EQUATIONS

Since the flow is transonic, it turns out to be convenient to normalize all basic state quantities to their values at the sonic radius. Letting an asterisk subscript indicate the values of a quantity at the sonic radius we introduce the following new variables:

$$\begin{aligned} r' &= r/r_*, \quad \theta = T/T_*, \quad p' = p/p_*, \quad \rho' = \rho/\rho_*, \\ v' &= v/v_*, \quad w' = v'^2, \quad q' = q/q_*, \quad E' = E/E_*, \\ \Lambda' &= \Lambda(E)/\Lambda(E_*), \quad L' = L(E)/E_* \Lambda(E_*). \end{aligned} \quad (11)$$

At the sonic radius,  $r=r_*$ , we have the obvious relations

$$\rho_* v_* r_*^2 = G/4\pi, \quad (12)$$

and

$$v_* = (\gamma k T_*/m)^{1/2}. \quad (13)$$

Introducing the new variables into Eqs. (4)–(7) and the equation of state, and dropping the primes for ease of notation yields, after some manipulation,

$$\frac{dw}{dr} = \frac{4w\theta}{\theta - w} \left( \frac{Q q_* r_* \sqrt{m} (\gamma - 1) \Lambda(E_*) q \Lambda}{2(\gamma k T_*)^{3/2} \theta \sqrt{w}} - \frac{1}{r} \right). \quad (14)$$

The ablation cloud must continuously accelerate if  $p \rightarrow 0$  as  $r \rightarrow \infty$ , therefore,  $dw/dr$  must be continuous and positive. Since at  $r=1$ ,  $\theta - w = 0$  the quantity in the large parentheses must also equal zero. This enforces a relationship between the dimensional quantities at the sonic radius giving, for  $kT_*$ ,

$$kT_* = \frac{2^{-2/3}}{\gamma} m^{1/3} [Q(\gamma - 1) q_* r_* \Lambda_*]^{2/3}. \quad (15)$$

With Eq. (15) the differential equations for  $w$ ,  $\theta$ ,  $q$ , and  $E$  can be written in a form suitable for numerical integration:

$$\frac{dw}{dr} = \frac{4w\theta}{(\theta - w)r} \left( \frac{q \Lambda(E)r}{\theta \sqrt{w}} - 1 \right), \quad (16)$$

$$\frac{d\theta}{dr} = \frac{2\Lambda(E)q}{\sqrt{w}} - \frac{1}{2}(\gamma - 1) \frac{dw}{dr}, \quad (17)$$

$$\frac{dE}{dr} = 2\lambda_* \frac{L}{r^2 \sqrt{w}}, \quad (18)$$

$$\frac{dq}{dr} = \lambda_* \frac{q \Lambda}{\sqrt{w} r^2}, \quad (19)$$

where the eigenvalue,  $\lambda_*$  is given by the dimensionless quantity

$$\lambda_* = \rho_* r_* \Lambda_* / m. \quad (20)$$

It is the only adjustable parameter that could alter the relationship between the dimensionless quantities in the

ablation cloud. Its value is determined in conjunction with the dimensionless pellet radius  $\hat{r} = r_p/r_*$ , by invoking the surface boundary conditions (10). Formally, we have

$$q_1(\lambda_*, \hat{r}) = 0, \quad \theta_1(\lambda_*, \hat{r}) = 0. \quad (21)$$

The unique integral curve for the kinetic energy  $w$ , passing through the singular point  $r=1$ , is found by first finding the value of the indeterminate derivatives,  $dw/dr|_{r=1}$ . Knowing this derivative, one can progress with the integrations of Eqs. (16)–(19) away from the singular point. Let  $dw/dr|_{r=1} = \chi_*$ . Applying l'Hospital's rule to Eq. (16), one finds that

$$\chi_* = \frac{\frac{1}{2}(3-\gamma) + \{[\frac{1}{2}(3-\gamma)]^2 - \frac{1}{2}(\gamma+1)(\lambda_* + \psi_*) - 1\}^{1/2}}{(\gamma+1)/4},$$

where

$$\psi_* = \frac{d\Lambda}{dr} \Big|_{r=1} = \frac{2\lambda_* L(E)}{\Lambda^2(E)} \frac{d\Lambda}{dE} \Big|_{E=E_*}.$$

The system of equations (16)–(19) is then integrated into the subsonic domain ( $r < 1$ ). We proceed until a point  $r = \hat{r}$  is reached such that the surface boundary conditions (21) are satisfied. This locates the pellet surface since  $r_p = \hat{r} r_*$ . If no such point exists, then a different  $\lambda_*$  is chosen. With  $\lambda_*$  correctly chosen, the solutions to Eqs. (16)–(19) are carried out for  $r > 1$  (the supersonic domain) until  $q$  and  $E$  approach their asymptotic values which are denoted by  $\hat{q} = q_0/q_*$  and  $\hat{E} = E_0/E_*$ , respectively. Note that the differential equations with the boundary conditions given here are universal, in that they need only be integrated once for a given selection of  $E_*$ :  $\hat{r}$ ,  $\hat{q}$ , and  $\lambda_*$  are functions of  $E_*$  alone, independent of  $q_*$  and  $r_*$ . The solutions, of course, correspond to a definite external plasma temperature since  $\hat{E} = E_0/E_* = 2kT_{e0}/E_*$ . Therefore, when we speak about the differential equations and the boundary conditions being independent of the energy flux  $q_0$ , for a given  $E_*$ , we actually mean they are independent of the density  $n_{e0}$ , since the temperature of the plasma is fixed.

The dimensionless parameters are displayed in Figs. 1 and 2 as a function of the external plasma temperature  $kT_{e0}$ . They are seen to be weak functions of  $T_{e0}$ . The dashed lines in these figures are values for  $\gamma = 1.4$  including the effect of the heat of vaporization for the pellet molecules. [This is only important for low plasma densities ( $n_{e0} < 10^{12}$ ) and small pellet radii ( $r_p < 0.005$  cm), parameters usually associated with low plasma temperatures.] A simple functional relationship can be obtained from the curves for  $\gamma = 5/3$  giving

$$\hat{E} = 1.25 - 0.0147 \ln E_0, \quad (22)$$

or

$$E_* = E_0 / \hat{E}, \quad (23)$$

$$\hat{q} = 1.516 - 0.004 \ln E_0, \quad (24)$$

$$\hat{r} = 0.696 - 0.0117 \ln E_0, \quad (25)$$

$$\lambda_* = 0.905 - 0.014 \ln E_0. \quad (26)$$

The dimensional quantities at the sonic radius  $v_*$ ,  $T_*$ ,  $\rho_*$ , and the ablation rate  $G$  can be found by solving Eqs.

(12), (13), (15), and (20). Using Eq. (1) and the definitions for the asymptotic quantities  $\hat{r}$ ,  $\hat{E}$ , and  $\hat{q}$  we obtain these dimensional quantities in terms of the pellet radius  $r_p$  (cm), plasma density,  $n_{e0}$  ( $\text{cm}^{-3}$ ), and temperature  $T_{e0}$  (eV) finally giving

$$T_* = 6.638 M_0^{1/3} \frac{(\gamma - 1)^{2/3}}{\gamma} \frac{(Q n_{e0} r_p)^{2/3}}{(\hat{r} \hat{q})^{2/3}} T_{e0} \Lambda^{2/3}(E_*) \text{ (eV)}, \quad (27)$$

$$v_* = \frac{2.52 \times 10^6}{M_0^{1/3}} (\gamma - 1)^{1/3} \frac{(Q n_{e0} r_p)^{1/3}}{(\hat{r} \hat{q})^{1/3}} \Lambda^{1/3}(E_*) \text{ (cm/sec)}, \quad (28)$$

$$\rho_* = \frac{1.67 \times 10^{-24} M_0 \lambda_* \hat{r}}{r_p \Lambda(E_*)} \text{ (g/cm}^3\text{)}, \quad (29)$$

$$p_* = 10.62 M_0^{1/3} \frac{(\gamma - 1)^{2/3}}{\gamma} \lambda_* \frac{\hat{r}^{1/3}}{\hat{q}^{2/3}} \frac{(Q n_{e0})^{2/3}}{r_p^{1/3}} \times T_{e0} \Lambda(E_*)^{-1/3} \text{ (dyn/cm}^2\text{)}, \quad (30)$$

and

$$G = 5.29 \times 10^{-17} M_0^{2/3} (\gamma - 1)^{1/3} \frac{\lambda_*}{\hat{r}^{4/3} \hat{q}^{1/3}} (Q n_{e0})^{1/3} \times r_p^{4/3} T_{e0}^{1/2} \Lambda(E_*)^{-2/3} \text{ (g/sec)}. \quad (31)$$

In Eqs. (27)–(31)  $M_0$  is the mass of the ablated molecule in amu, e.g.,  $M_0=4$  for  $D_2$ .

The pellet surface regression speed,  $\dot{r}_p$ , is

$$\dot{r}_p = G / 4\pi m n_0 r_p^2, \quad (32)$$

where  $n_0$  is the molecular number density of the solid pellet. Combining Eqs. (31) and (32) gives

$$\dot{r}_p = 2.52 \times 10^6 \frac{(\gamma - 1)^{1/3}}{n_0 M_0^{1/3}} \frac{\lambda_*}{\hat{r}^{4/3} \hat{q}^{1/3}} \frac{(Q n_{e0})^{1/3}}{r_p^{2/3}} T_{e0}^{1/2} \Lambda(E_*)^{-2/3} \quad (33)$$

Since quasi-steady conditions prevail, the ablation rate is a function of the instantaneous pellet radius. Using

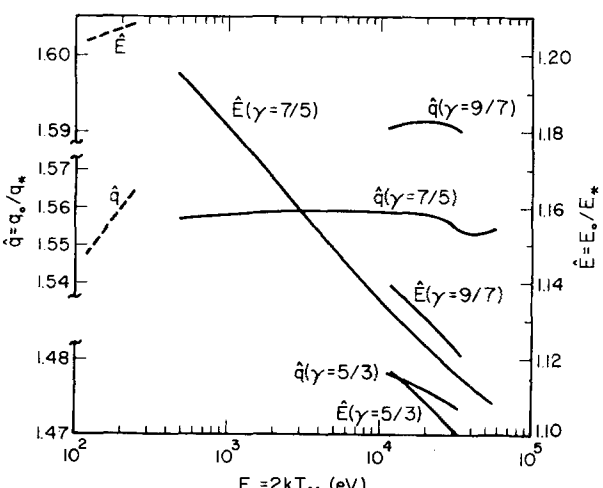


FIG. 1. Ratio of the plasma electron energy and energy flux to the electron energy and energy flux at the sonic surface,  $\hat{E}$  and  $\hat{q}$ , as a function of the plasma electron temperature.

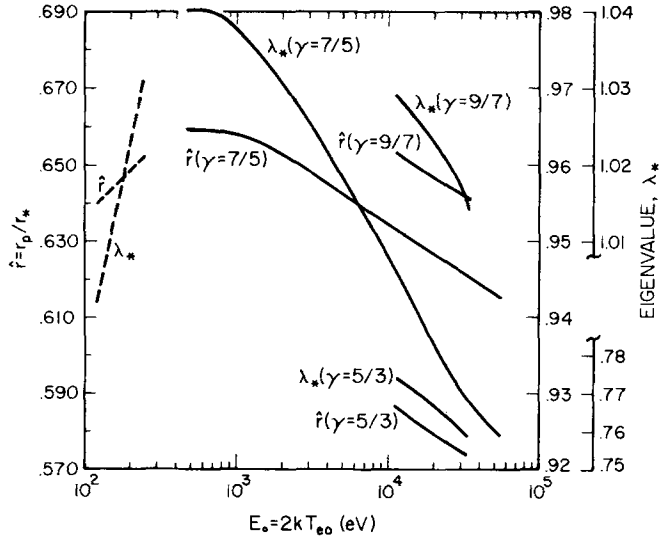


FIG. 2. Ratio of the pellet radius to the sonic radius,  $\hat{r}$ , and eigenvalue,  $\lambda_*$ , as a function of the plasma electron temperature.

Eq. (33), the lifetime  $\tau_p$  of a pellet of initial radius  $r_{p0}$  (for steady plasma conditions) becomes

$$\tau_p = \frac{2.38 \times 10^{-7}}{(\gamma - 1)^{1/3}} n_0 M_0^{1/3} \frac{\hat{r}^{4/3} \hat{q}^{1/3}}{\lambda_*} \frac{r_{p0}^{5/3} \Lambda^{2/3}(E_*)}{(Q n_{e0})^{1/3} T_{e0}^{1/2}}. \quad (34)$$

If the average particle mass,  $m$ , in the ablation cloud is closer to the atomic mass rather than the molecular mass, then the quantities  $M_0$ ,  $\Lambda(E_*)$ , and  $n_0$  should be replaced by  $M_0/2$ ,  $\Lambda(E_*)/2$ , and  $2n_0$ , respectively. If this is done in Eqs. (33) and (34), they will be left unchanged except for  $T_*$  which becomes  $T_*/2$ .

The basic state profiles  $v$ ,  $w$ ,  $\theta$ ,  $p$ ,  $q$ ,  $E$ , and the Mach number  $M=(w/\theta)^{1/2}$  are almost identical for the various  $E_*$ 's selected. Figures 3 and 4 display profiles for  $E_*=30$  keV ( $T_{e0}=16.7$  keV) and  $\gamma=1.4$ . The pellet radius with respect to the sonic radius is located at  $r=\hat{r}=0.621$ . At  $r=\hat{r}$ , the pressure in the ablation cloud is at its maximum and falls continuously; its value with respect to  $p_*$  is 3.5. At  $r=\hat{r}$ , the dimensionless energy flux  $q$  is essentially zero and the dimensionless average electron energy  $E$  is 15% of its value at  $r=1$ . This is quite reasonable since scattering dominates slowing down in the energy flux degradation process, i.e.,

$$\frac{\hat{\sigma}_t(E_*)}{2L(E_*)/E_*} \text{ is about } 3,$$

which means that the average electron energy does not have to go to zero when the energy flux does. As can be seen, most of the energy flux is absorbed in the vicinity of the sonic surface; in fact, about one-third of the energy flux is absorbed in the supersonic portion of the ablation cloud, whereas two-thirds is absorbed in the subsonic portion, about 95% is absorbed within four sonic radii. (The pellet, in fact, absorbs only a minuscule fraction of the total electron energy flux which goes into vaporization.) The low Mach number in the supersonic region is due to the expansion into a background of essentially constant energy flux. Heat addition is always present to compete against the effects of radial

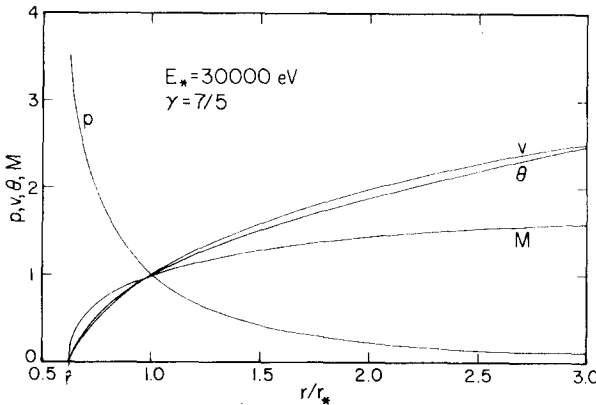


FIG. 3. Dimensionless pressure,  $p$ , flow velocity,  $v$ , temperature,  $\theta$ , and Mach number,  $M$ , in the ablation cloud versus dimensionless coordinate  $r/r_*$  for a plasma electron temperature of 30 keV. The surface of the pellet is located at  $r = 0.6215$ , and the dimensionless pressure of the ablation cloud at the surface is 3.508.

expansion. In an adiabatic flow, where only radial expansion is in operation, the Mach number increases without limit.

It can be shown analytically, from Eqs. (16) and (17), that the asymptotic expressions for  $v(r)$ ,  $\theta(r)$ , and  $p(r)$  and the Mach number  $M$ , for  $r \rightarrow \infty$  are

$$v_\infty(r) = \left( \frac{30\hat{\Lambda}\hat{q}}{7\gamma - 5} \right)^{1/3} r^{1/3}, \quad \theta_\infty(r) = \frac{\gamma}{5} \left( \frac{30\hat{\Lambda}\hat{q}}{7\gamma - 5} \right)^{2/3} r^{2/3}, \quad (35)$$

$$p_\infty(r) = \frac{\gamma}{5} \left( \frac{30\hat{\Lambda}\hat{q}}{7\gamma - 5} \right)^{1/3} r^{5/3}, \quad M_\infty = \left( \frac{5}{\gamma} \right)^{1/2}.$$

The change in  $\gamma$  was not found to be particularly significant as far as the effect on the pellet lifetime is concerned. In summary, the lifetimes for different  $\gamma$ 's are found to have their ratios  $\tau_p(\gamma = 5/3): \tau_p(\gamma = 7/5): \tau_p(\gamma = 9/7)$  proportional to 1:1.0884:1.1692 (in these calculations  $T_{e0} = 14$  keV).

Before concluding this section, it is shown that a very physical interpretation of the eigenvalue  $\lambda_*$  can be found in connection with the range-limiting behavior of the ablation cloud. (The integrated cloud thickness is such as to completely adsorb the energy flux.) For a given  $\gamma$ , one can see from Fig. 2 [or Eq. (26)] that  $\lambda_*$  is fairly constant for a wide range of plasma temperatures. According to Eq. (20),  $(\rho_*/m)\lambda_*$  is, therefore, nearly invariant for any plasma temperature. Thus, increasing the pellet radius (which increases  $r_*$ ) causes the density of the ablation cloud to drop in order to maintain the range limiting thickness. Similarly, increasing the range of the plasma electrons (decreasing  $\Lambda_*$ ) leads to an increase in the ablation cloud density for a given  $r_p$ . In addition,  $\lambda_*$  can be seen to be physically invariant under plasma density changes. Increases in the plasma density cause the ablation rate to increase slightly. Simultaneously, the ablation cloud expansion velocity is driven up due to the increased heating. These effects cancel one another leaving  $\rho_*$

constant. The "range-limited" concept is similar in principle to Krokhin's<sup>12</sup> self-matched regime where the optical thickness of materials heated by intense laser light tends to remain at a constant value throughout the course of heating. In our case, though, the pellet radius in a manner of speaking, determines the "optical thickness."

#### IV. SCALING LAWS AND COMPARISON WITH EXPERIMENT

For hydrogen pellets Eqs. (28), (29), (30), (33), and (34) can be expressed in the form of simple scaling laws for plasma temperature in the range 1–30 keV. With  $Q = 0.65$  and  $\gamma = 7/5$  these equations take the form

$$T_* = 1.12 \times 10^{-8} r_p^{2/3} n_{e0}^{2/3} T_{e0}^{-0.14} \text{ eV}, \quad (36)$$

$$v_* = 86.6 r_p^{1/3} n_{e0}^{1/3} T_{e0}^{-0.07} \text{ cm/sec}, \quad (37)$$

$$\rho_* = 7.36 \times 10^{-12} r_p^{-1} T_{e0}^{1.68} \text{ g/cm}^3, \quad (38)$$

$$p_* = 3.95 \times 10^{-8} r_p^{-1/3} n_{e0}^{2/3} T_{e0}^{1.54} \text{ dyn/cm}^2, \quad (39)$$

$$\dot{r}_p = 1.72 \times 10^{-8} r_p^{-2/3} n_{e0}^{1/3} T_{e0}^{1.64} \text{ cm/sec}, \quad (40)$$

$$\tau_p = 3.47 \times 10^{-7} r_p^{5/3} n_{e0}^{-1/3} T_{e0}^{-1.64} \text{ sec}. \quad (41)$$

Solid deuterium and tritium have slightly higher solid molecular number densities,  $n_0$ , and molecular masses,  $M_0$ , than hydrogen so that the pellet lifetime would be increased by a factor of 1.43 for a pellet composed of deuterium and by a factor of 1.62 for a pellet composed of an equal mixture of D and T.

In order to compare the results of this theory with the pellet injection experiments done on ORMAK,<sup>13</sup> the following parameters are used. Since the plasma temperature is low (about 100 eV), a low energy approximation for the electron scattering and energy loss which is appropriate is

$2L(E)/E + \sigma_t(E) \approx 4.36 \times 10^{-14} E^{-1.19} \text{ cm}^2$ . From Figs. 1 and 2 (the dashed lines)  $\lambda_* = 0.94$ ,  $\hat{r} = 0.64$ ,  $\hat{q} = 1.55$ , and  $\hat{E} = 1.2$ . For temperature and density profiles in the plasma we assume linear relations from the limiter to a point 7.4 cm into the plasma. At 7.4 cm into the plasma the density is  $7 \times 10^{12} \text{ cm}^{-3}$  and the electron tem-

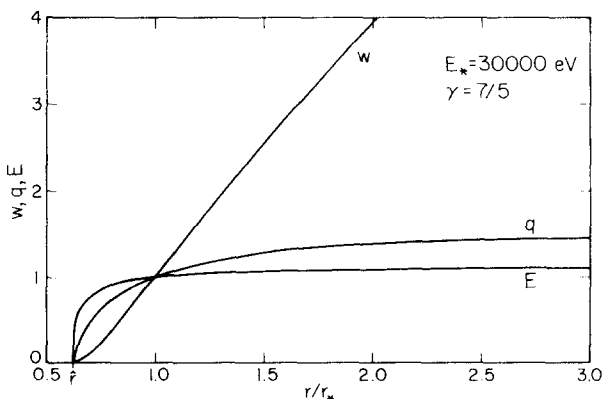


FIG. 4. Dimensionless kinetic energy of flow,  $w$ , electron energy flux,  $q$ , and average electron energy,  $E$ , in the ablation cloud versus dimensionless coordinate  $r/r_*$  for a plasma electron temperature of 30 keV.

perature is 175 eV. At the limiter the density is  $3.7 \times 10^{11} \text{ cm}^{-3}$  and the temperature is 10 eV. Under these assumptions the lifetime of a pellet of radius 105  $\mu\text{m}$ , traveling at 100 m/sec into the plasma at a 45° angle, is calculated to be 1040  $\mu\text{sec}$  as compared with the average experimental value of 880  $\mu\text{sec}$ .<sup>13</sup> (These numbers assume that the measured light output starts when the pellet is 2 cm outside the limiter but that the ablation is negligible before the pellet reaches the limiter.) This is well within the error in the pellet lifetimes and the plasma density and temperature profiles which are not that well known near the limiter.

In order to calculate the penetration of a pellet into a hot plasma, Eq. (40) can be used along with the temperature and density profile of the plasma. For example, for a linear temperature and density profile the lifetime depends on the pellet radius to the 0.56 power rather than the 5/3 power as in the case of constant plasma conditions [Eq. (41)]. Pellet lifetimes in colder plasmas can be found with different approximations for the scattering and energy loss functions as was done for the ORMAK experiments.

Using the results of Eq. (40) projections can be made of the velocity a pellet needs to penetrate into a reactor. Calculations were done for the experimental power reactor designed by General Atomic Company and the UWMAK-III reactor designed by the University of Wisconsin. The pellets were composed of equal parts of deuterium and tritium, contained 10% of the total mass of the plasma and traveled along a minor radius. Approximations were made to the temperature and density profiles. For the General Atomic experimental power reactor the electron temperature profile was  $12.8(1 - r/a)^{0.25}$  keV, where  $r$  is the distance from the magnetic axis of the reactor and  $a$  is the minor radius. A uniform electron density of  $1.6 \times 10^{14} \text{ cm}^{-3}$  was assumed. For this reactor then  $r_p = 0.57 \text{ cm}$ . Penetration to the magnetic axis can be achieved if the pellet velocity is  $1.1 \times 10^6 \text{ cm/sec}$  and halfway to the magnetic axis if its velocity is  $4 \times 10^5 \text{ cm/sec}$ . For the UWMAK-III the same quantities were electron temperature  $20(1 - r/a)$  keV, electron density  $3 \times 10^{14}(1 - r/a) \text{ cm}^{-3}$ , pellet radius 0.90 cm, velocity for full penetration  $1.5 \times 10^6 \text{ cm/sec}$ , and velocity for half-penetration  $1.9 \times 10^5 \text{ cm/sec}$ . The conclusion from this is that if one wants to refuel fusion reactors in the center of the plasma, the technology of accelerating pellets to  $10^6 \text{ cm/sec}$  should be developed.

When these results for the pellet lifetime are compared with the earlier sonic flow approximation model,<sup>2</sup> it is found that the transonic-flow model predicts pellet lifetimes which are about 25%–30% lower, although the scaling laws for both models are essentially the same. In the earlier model the authors made two simplifica-

tions in order to obtain an analytic solution of the spherical gasdynamic equations. First, the Mach number was set equal to one at all radii. Second, the product  $q\Lambda(E)$  in the heat flow equation was taken to be constant [ $q\Lambda(E) = q_0\Lambda(E_0)$ ] at all radii.

## V. CONCLUSION

The ablation rate for a solid hydrogen pellet exposed to a plasma has been obtained by solving the spherical gas dynamic equations in conjunction with a transport equation for the incident electron energy flux. Because the thickness of the ablation cloud and its rapidity of expansion govern the ablation rate rather than the details of the phase transition at the pellet surface, we have analyzed the ablation cloud flow at the sonic radius and have found that the equations are invariant for plasma density and pellet radius. The various basic state quantities at the sonic radius of the flow as well as an expression for the pellet surface regression speed and lifetime can be expressed by fairly simple expressions for  $n_{e0}$ ,  $T_{e0}$ , and  $r_p$ .

## ACKNOWLEDGMENTS

This paper is based in part on a dissertation by one of us (P. B. P.) in partial fulfillment of the requirement for the Ph. D. at the University of Illinois, Urbana, Illinois.

This work was supported in part by the U.S. Energy Research and Development Administration under Contract No. EY-76-S-02-2234.

- <sup>1</sup>J. W. Davis and G. L. Kulcinski, Nucl. Fusion **16**, 355 (1976).
- <sup>2</sup>P. B. Parks, R. J. Turnbull, and C. A. Foster, Nucl. Fusion **17**, 539 (1977).
- <sup>3</sup>A. H. Shapiro, *The Dynamics and Thermodynamics of Compressible Fluid Flow* (Ronald Press, New York, 1973), p. 93.
- <sup>4</sup>S. J. Gitomer, R. L. Morse, and B. S. Newberger, Phys. Fluids **20**, 234 (1977).
- <sup>5</sup>P. B. Parks, Ph. D. dissertation, University of Illinois (1977).
- <sup>6</sup>P. B. Parks and F. S. Felber (to be published).
- <sup>7</sup>R. Radtke and K. Gunther, J. Phys. D **9**, 1131 (1976).
- <sup>8</sup>G. M. N. Saha, Philos. Mag. **40**, 472 (1920).
- <sup>9</sup>H. T. Malcker, H. Schenk, and W. J. Peters, Z. Phys. **140**, 119 (1955).
- <sup>10</sup>H. G. Heaps, and A. E. S. Green, J. Appl. Phys. **46**, 4718 (1975).
- <sup>11</sup>W. T. Miles, R. Thompson, and A. E. S. Green, J. Appl. Phys. **43**, 678 (1972).
- <sup>12</sup>O. N. Krokhin, Zh. Tekh. Fiz. **34**, 1324 (1964) [Sov. Phys.-Tech. Phys. **9**, 1024 (1965)].
- <sup>13</sup>C. A. Foster, R. J. Colchin, S. L. Milora, K. Kim, and R. J. Turnbull, Nucl. Fusion **17**, 1067 (1977).